

Monolayers and Langmuir–Blodgett Films of a Newly Synthesized Asymmetric Tetraazaporphyrin Derivative

Francesca Bonosi,[†] Giampaolo Ricciardi,[‡] Francesco Leij,[‡] and Giacomo Martini^{*,†}

Dipartimento di Chimica, Università di Firenze, 50121 Firenze, Italy, and Dipartimento di Chimica, Università della Basilicata, 85100 Potenza, Italy

Received: April 5, 1994; In Final Form: June 30, 1994[®]

Molecular assemblies such as monolayers at the water–air interface and Langmuir–Blodgett films of 2,3-bis(*N*-(3-thiopropyl)phthalimido)–7,8,12,13,17,18-hexakis(octylthio)–5,10,15,20-tetraazaporphyrinato (TAP) copper(II) and nickel(II) derivatives were studied for the first time. Monolayers at the water–air interface both of the pure macrocyclic derivative and of its mixture with stearic acid were investigated. The degree of order within Langmuir–Blodgett films was established with the aid of UV–vis and ESR spectroscopies. The surface behavior of the above unsymmetrically substituted TAP, in the form of metal derivatives, has been compared with that of the corresponding symmetrically substituted compounds (Bonosi; *et al. J. Phys. Chem.* 1993, 97, 9181), which give disordered films. We report here on the improved ordering in the LB film fabrication reached with the unsymmetrical substitution as being due to the presence of the hydrophilic phthalimide moieties in two of the eight long chains around the TAP skeleton, which favor an edge-on orientation of the macrocycle at the air–water interface.

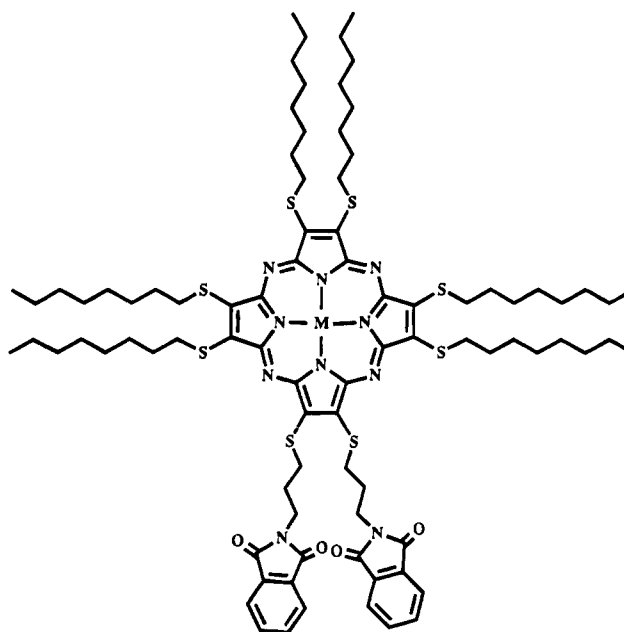
Introduction

Highly ordered Langmuir–Blodgett films of tetraazamacrocyclic rings, such as porphyrins, tetraazaporphyrins, and phthalocyanines, are desirable for both fundamental and applied studies because of their interesting optical, magnetic, and electrical properties.^{1–3}

In particular, tetraazaporphyrins (TAP), also known as porphyrazines, are aromatic macrocycle compounds composed of four pyrrole rings bridged by four aza nitrogen atoms, which may be used as amphiphilic material for thin film fabrication. They are also very suitable for metal ligation and have unique optical, electric, and catalytic properties, although they have not been investigated as widely as other azamacrocycles. This is most probably due to the lack of efficient syntheses of soluble derivatives. Transition metal complexes of symmetrically substituted TAP are known to give thermotropic columnar liquid crystals, i.e. discotic mesophases that are stable over a wide range of temperatures^{4,5} as well as other metal alkyl-substituted porphyrins.^{5–8}

In a previous study⁹ we investigated the monolayer properties and the LB film deposition of some mesogenic highly symmetric derivatives of the tetraazaporphyrin core. These symmetric molecules as pure compounds do not form true monomolecular layers, and thus they cannot be deposited as Langmuir–Blodgett films. A better film transfer is obtained when the TAP molecules are diluted in an amphiphilic host matrix of stearic acid, but a good molecular ordering is not achieved. As a result of this finding, we decided to change the lateral substitution pattern in the TAP core. The combination of hydrophobic and hydrophilic chains is predicted to favor molecular ordering at the water–air interface.^{1–3} Furthermore, it is well documented that an asymmetric substitution pattern induces an edge-on orientation of the macrocycles at the water–air interface.^{1–3,10–13} With this aim we synthesized a new asymmetric tetraazaporphyrin (TAP) skeleton containing two *N*-(3-thiopropyl)phthalimide substituents in the 2 and 3 positions and six octylthio groups in the 7, 8, 12, 13, 17, and 18 positions:

M = H₂, Ni, Cu



2, 3-di-*N*-(3-thiopropyl)phthalimide, 7, 8, 12, 13, 17, 18-hexa-(octylthio) 5, 10, 15, 20 tetraazaporphyrin
(MR₆R₂'TAP)

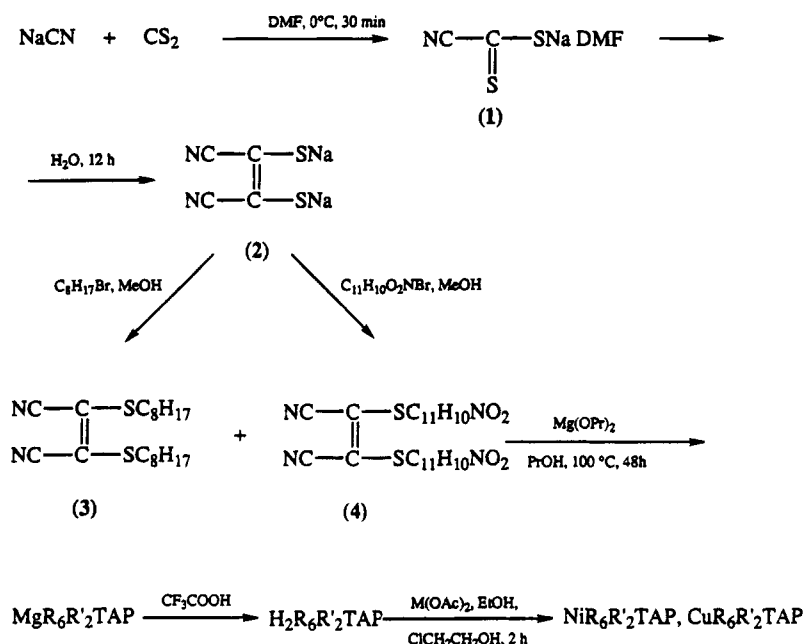
The presence of the straight long chain alkyl groups improves the solubility of the TAP core in the organic spreading solvent and enhances chain–chain intermolecular interactions, whereas the hydrophilic substituents favor an ordered orientation of the molecules at the water–air interface and in the transferred films. The free base and the copper(II) and nickel(II) derivatives have been prepared.

In the present work we studied monolayers and LB films of the above asymmetric compounds. The properties of the monolayers were investigated from their π/A isotherms, from their stability as a function of time, and from the compression–expansion–compression cycles. ESR spectroscopy and UV–

[†] Università di Firenze.

[‡] Università della Basilicata.

[®] Abstract published in *Advance ACS Abstracts*, September 1, 1994.

SCHEME 1^a

^a Attention must be paid when handling NaCN and CS₂ reagents.

vis spectroscopy in isotropic and polarized light were used in order to determine the molecular order degree.

Experimental Section

Materials. All materials used in this work were reagent grade. Stearic acid (SA) and CdCl₂ were supplied by Sigma. KHCO₃ was supplied by Merck. All chemicals used for the syntheses of the new asymmetric tetraazaporphyrin were of reagent grade (Aldrich) and used without further purification.

Syntheses. The metal free tetraazaporphyrin, H₂R₆R'₂TAP, was prepared by a modification of the method used by Schramm and Hoffmann¹⁴ for the synthesis of octakis(methylthio)-tetraazaporphyrin, starting from compound 1 (see Scheme 1). Disodium *cis*-1,2-dicyano-1,2-ethylenedithiolate (2) and 1,2-dicyano-1,2-bis(octylthio)ethylene (3) were prepared following the procedure reported in the literature.¹⁴

Preparation of 1,2-Dicyano-1,2-bis(*N*-(3-thiopropyl)phthalimido)ethylene (4). To a vigorously stirred suspension of 1 (1 g, 5.4 mmol) in 10 mL of methanol was added *N*-(3-bromopropyl)phthalimide (2.9 g, 10.9 mmol) over a period of 1 h at room temperature. After 24 h, the reaction was completed and the compound 4 separated as yellow platelets. The solid was filtered off, washed with water and methanol, and crystallized from methanol/diethyl ether. Yield: >95%.

¹H-NMR (CDCl₃, TMS as internal standard): δ = 2.1–3.4 (8H, N-CH₂ and S-CH₂); 3.85 dt (4H, -(CH₂)-); 7.65, 7.80 m (8H, aromatic ring).

IR: 2735 cm⁻¹ (strong), -CN stretch; 1675 cm⁻¹ (strong), -CO stretch.

MgR₆R'₂TAP. Mg powder (0.400 g, 1.66 mmol) washed with diethyl ether and air dried was refluxed 12 h in 50 mL of *n*-propanol. 3 (2.7 g, 0.74 mmol) was added under stirring to the boiling suspension. 4 (1.6 g, 0.25 mmol) was further added to the suspension when this turned deeply green. The reaction vessel was kept under mild reflux for 48 h. After cooling, the dark blue and dense slurry was extracted with acetone. The resulting solution, after removal of the solvent under vacuum, afforded a precipitate that was washed with acidulated water (HCl) and diethyl ether and then air dried. Further purification

by column chromatography (silica gel, Merck 9385 230/400 mesh, chloroform) led to about 3 g of product.

H₂R₆R'₂TAP. The mixture of isomers and variously substituted Mg-tetraazaporphyrins was dissolved in the minimum amount of CF₃COOH and carefully poured into an ice/water bath. The solution was neutralized with concentrated ammonia. The resulting dark solid, separated by filtration and dissolved in CH₂Cl₂, was shaken in a separatory funnel with several portions of water until neutrality. After removal of the solvent, the dark solid was dried over P₂O₅. H₂R₆R'₂TAP was isolated by flash chromatography on silica gel using as eluent a 1/1 mixture of hexane/dichloromethane (*R_f* = 0.75 at *T* = 20 °C; second band). A yield on the order of 30% has been calculated on the basis of the isomer mixture. The product, having the shape of thin metallic needles, was characterized by the following:

¹H-NMR (CDCl₃, TMS as internal standard): δ = -0.1 (2H, -NH), 1.15–1.25 t (18H, -CH₃), 5.00–5.30 s (12H, S-CH₂), 3.00–3.48 t (4H, S-CH₂), 1.60–2.80 m (84H), 8.4–8.7 m (8H, aromatic rings).

IR: in addition to the usual absorptions of the TAP core in the region 1200–1500 cm⁻¹, 3280 cm⁻¹, -NH stretch; 1710 cm⁻¹, -CO stretch; 555 cm⁻¹, C-S-CH₂- stretch; 650–750 cm⁻¹, fingerprint of *ortho*-substituted benzene.

Analytical data calc for C₈₆H₁₂₄N₁₀O₄S₈: C, 63.82; H, 7.72; N, 8.65; O, 3.95; S, 15.84. Found: C, 63.68; H, 7.84; N, 8.40; O, 3.80; S, 16.01.

MR₆R'₂TAP (M = Ni, Cu). NiAc₂·4H₂O (CuAc₂·2H₂O) (0.020 g, 0.08 mmol), dissolved in 5 mL of hot ethanol, was added dropwise to a boiling solution of 0.100 g (0.05 mmol) of H₂R₆R'₂TAP in 20 mL of 2-chloroethanol. The mixture was stirred and kept under reflux for 2 h (the progress of the reaction was monitored by UV-vis spectroscopy). After cooling, dark needles separated from the solution. These were collected by filtration, washed with ethanol, and air dried. Pure products were obtained by column chromatography (silica gel, dichloromethane) (*R_f* = 0.65 and 0.58 for NiR₆R'₂TAP and CuR₆R'₂TAP, respectively, on silica gel, 1/1 hexane/dichloromethane, *T* = 20 °C). Yield >90%.

The mixed Ni(II)/Cu(II) compound (38/1 atomic ratio) was prepared from the appropriate amounts of chloroform solutions of the copper and nickel compounds. The mixture was evaporated to dryness under stirring, and the resulting solid was taken without further treatment.

Techniques. The spreading isotherms at 293 K of all the studied systems were determined with a Lauda FW1 film balance, using a step-by-step compression, with a waiting time of 90 s between successive steps.

Stability curves were determined with the KSV LB5000 ALT apparatus.

The compression–expansion–compression cycles at 293 K were determined with a Lauda FW2 film balance using a continuous compression at 5 mm/min.

LB film deposition was performed with the KSV LB5000 ALT apparatus by using the following experimental conditions:

	π_{dipp} (mN/m)	v_{dipp} (mm/min)
Cu/NiR ₆ R' ₂ TAP 1/38	19	2
SA/CuR ₆ R' ₂ TAP 22/1	20	2

In order to improve the deposition, hydrophobic quartz slides were used, prepared by overnight immersion of accurately cleaned hydrophilic quartz plates in a 10% (v/v) solution of dimethyldichlorosilane in 1,1,1-trichloroethane, kept in an oven at 483 K for about 1 h and then carefully rinsed with acetone, chloroform, and twice-distilled water.

Twice-distilled water, purified with a MilliQ-water system (Millipore) up to a resistivity greater than 18 MΩ·cm, was used for the subphase preparation.

The electronic spectra were recorded with a Perkin-Elmer Lambda5 UV–vis spectrophotometer; *s*- and *p*-polarized light was obtained with the aid of two Polaroid sheet polarizers in the 350–800 nm range.

The ESR spectra were recorded using the Bruker 200D ESR spectrometer operating in the X band and interfaced with an IBM-AT computer. Data acquisition and treatment were carried out with the ESR software commercialized by Stelar S.p.a.

¹H-NMR spectra were recorded on a 300 MHz Bruker AM-300 spectrometer with (CH₃)₄Si as internal standard.

Elemental analyses were performed at the Department of Engineering, University of Basilicata.

Results and Discussion

Pure Compounds. The electronic spectra of chloroform solutions of both free base (3.5×10^{-7} M) and its copper derivative (1.3×10^{-7} M) are reported in Figure 1. The change of symmetry, from *D*_{4h} for the symmetrically substituted ring^{5,8,9} to *C*_{2v} for the asymmetric macrocycle, had a relatively small effect on the energy levels associated with the electronic transitions. The resulting spectra (whose assignment is described in the literature¹⁵) were typical of the tetraazamacrocyclic rings. The spectrum reported in Figure 1 closely resembled those reported for symmetrically substituted TAP,⁹ with the Soret band at 329 nm, a band at about 500 nm, which is due to an *n* → *π** type transition, and the Q band at 670 nm with a shoulder at higher energy (610 nm). The asymmetrical shape of the Soret band clearly indicated the overlapping of two different lines, due to two different transitions between the electronic levels. The latter was the only visible effect of the decreasing symmetry with respect to the symmetric compound.

The room temperature ESR spectrum of pure CuR₆R'₂TAP powder was a single, exchange-narrowed line with a peak-to-peak separation of 3.9 mT, to be compared with 4.1 mT for CuR₆TAP.⁹ The latter compound gives two marked disconti-

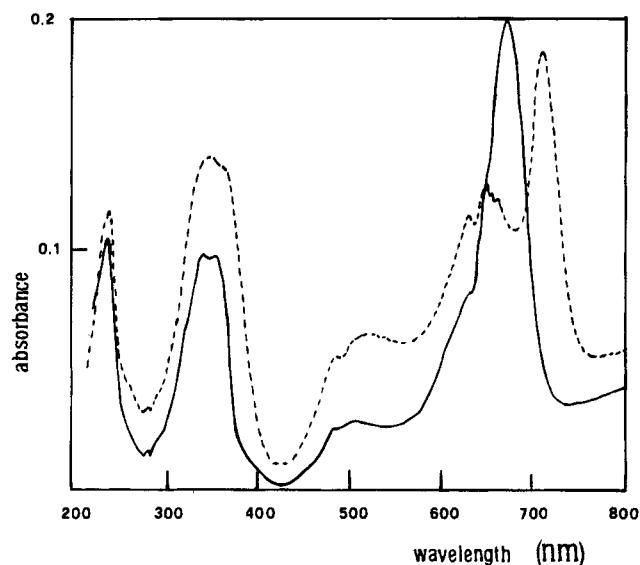


Figure 1. Electronic spectra at room temperature of CHCl₃ solutions of CuR₆R'₂TAP (1.3×10^{-7} mol/L, solid line) and of H₂R₆R'₂TAP (3.5×10^{-7} mol/L, dashed line).

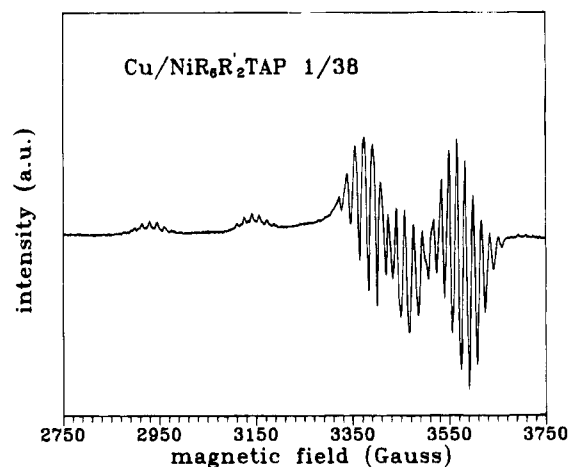


Figure 2. 297 K ESR spectrum of CuR₆R'₂TAP diluted (1/38 atomic ratio) in NiR₆R'₂TAP.

nities of the line width as a function of temperature, which reflect the solid → liquid crystal → isotropic liquid phase transitions typically shown by mesogenic substances. In contrast, CuR₆R'₂TAP gave only one discontinuity at 355 K, in the range 290–460 K, which probably ruled out a solid/liquid crystal phase transition in the above temperature range. This point was however beyond the interest of the present work, and it was not further investigated.

As previously done with the symmetric Cu-TAP derivative,⁹ the ESR spectrum of CuR₆R'₂TAP was studied for the compound magnetically diluted (1/38 atomic ratio) in the analogous Ni(II) compound. Figure 2 shows the pattern obtained with this mixture. The spectrum was typical of copper derivatives of macrocyclic compounds,¹⁶ with the copper ion coordinated in a square planar geometry by four equivalent nitrogen atoms. The lines at lower field, which are two of the four parallel components of the spectrum, show a partial resolution of the ¹⁴N hyperfine structure. The ¹⁴N superhyperfine structure was partially resolved on both parallel and perpendicular components of the powder spectrum. This was almost completely superimposable over the spectrum of Cu(II) in symmetrically substituted TAP,⁹ with the major difference being in the larger line widths which prevented the ⁶³Cu–⁶⁵Cu isotope line separation and introduced larger uncertainties in the line

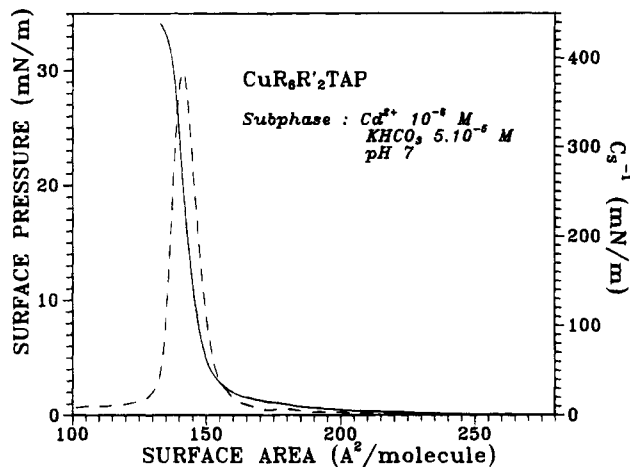


Figure 3. Spreading isotherm ($T = 293$ K) of $\text{CuR}_6\text{R}'_2\text{TAP}$ on a $\text{CdCl}_2/\text{KHCO}_3$ aqueous subphase (solid line) and compressibility modulus of the same system (dashed line).

positions. The same ESR parameters as for CuR_8TAP were therefore assumed, which are in good agreement with those reported for similar compounds.^{16–21}

Monolayers at the Water–Air Interface. The spreading behavior of the asymmetric tetraazaporphyrin was regular and aggregation phenomena were not observed, thus differing from octakis(alkylthio)tetraazaporphyrins,⁹ which are characterized by the formation of microcrystallites at the water–air interface, rather than a true monomolecular layer. The asymmetric substitution with two lateral chains containing two hydrophilic phthalimide groups positively favored the formation of a true monolayer. The 293 K π/A isotherm of undiluted $\text{CuR}_6\text{R}'_2\text{TAP}$, on a subphase containing cadmium ions, is reported in Figure 3. The observed limiting area value (A_0) of $147 \text{ \AA}^2/\text{molecule}$ was due to molecules perpendicularly orientated at the interface with the phthalimide moieties anchored to the water surface and the aliphatic side chains protruding toward the air phase. The measured value was indeed too low for a flat orientation of the molecules. The collapse pressure was about 29 mN/m . In addition, the value of 384 mN/m as a maximum in the surface compressional modulus, whose trend is also shown in the Figure 3, was indicative of a liquid phase at the water–air interface.

We also studied the $\text{Cu/NiR}_6\text{R}'_2\text{TAP}$ 1/38 mixture, in which the paramagnetic Cu(II)-TAP was diluted into the isomorphous diamagnetic nickel(II)-TAP compound. This mixture was used for ESR spectra (see above). The π/A isotherm of the mixture was very similar to that of the copper derivative, and the same A_0 value was calculated within experimental error. Thus, the presence of the nickel derivative did not affect the interfacial behavior. All the other measurements of monolayer properties were therefore performed on this system.

The stability of the monolayer at the surface pressure which was chosen for the LB film deposition (see below) was monitored by measuring the variation of surface area as a function of time (Figure 4). The $\text{Cu/NiR}_6\text{R}'_2\text{TAP}$ 1/38 monolayer showed an area decrease of less than 1% in 4 h. The monolayer was thus very stable and it can be said that neither solubilization of the molecules in the subphase nor molecular arrangement phenomena occurred.

Figure 5 shows the π/A isotherm of the $\text{Cu/NiR}_6\text{R}'_2\text{TAP}$ 1/38 system in compression–expansion–compression cycles, with the first compression up to 19 mN/m . A slight hysteresis was observed, indicating a not completely reversible behavior of the monolayer. The second compression isotherm had lower surface

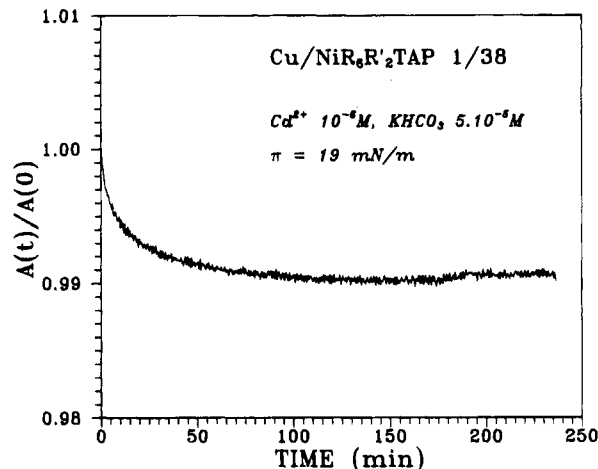


Figure 4. Stability of the $\text{Cu/NiR}_6\text{R}'_2\text{TAP}$ monolayer expressed as the decrease of the area ratio $A(t)/A(0)$ as a function of time ($T = 297$ K; $\pi = 19 \text{ mN/m}$).

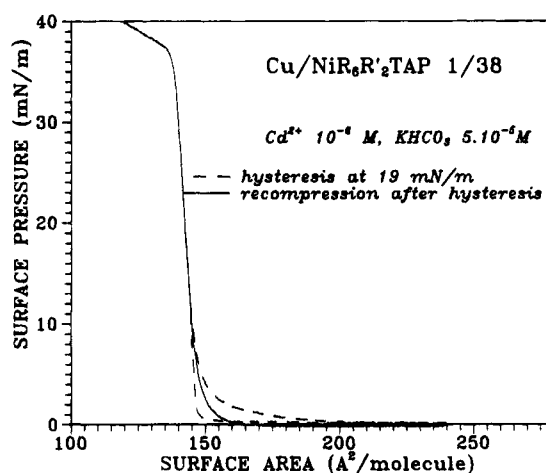


Figure 5. Compression–expansion–compression cycles of the $\text{Cu/NiR}_6\text{R}'_2\text{TAP}$ monolayer on the same subphase as in Figure 4.

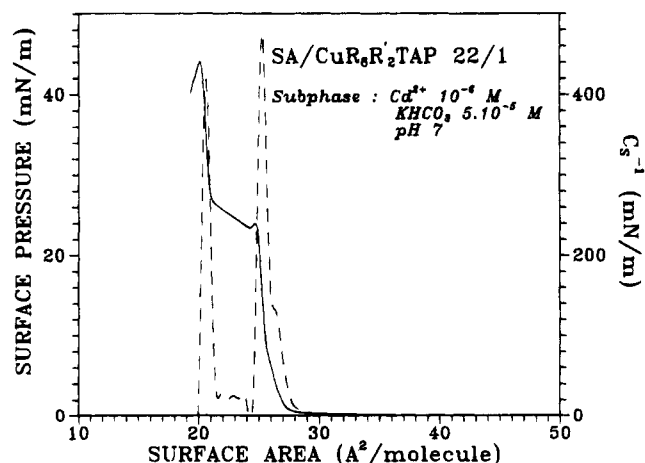


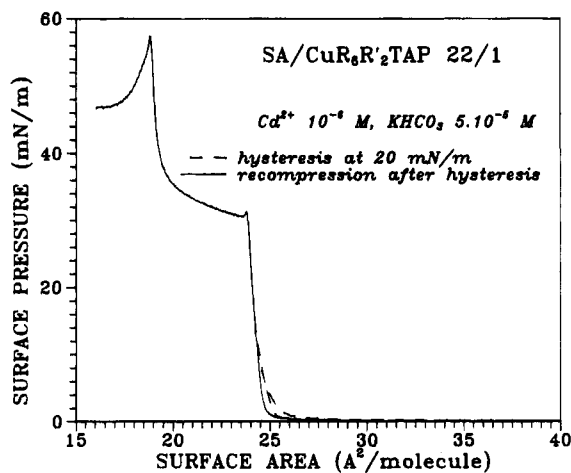
Figure 6. Spreading isotherm ($T = 293$ K, solid line) and compressibility modulus (dashed line) of the system $\text{SA/CuR}_6\text{R}'_2\text{TAP}$ (molecular ratio 22/1) on a water subphase containing $10^{-6} \text{ mol/L Cd}^{2+}$ and $5 \times 10^{-5} \text{ mol/L KHCO}_3$.

area values up to a surface pressure of 8 mN/m . Above this value we obtained a good overlapping of the two isotherms.

We also studied the stearic acid ($\text{SA/CuR}_6\text{R}'_2\text{TAP}$) system, in a 22/1 molecular ratio. The π/A isotherm (Figure 6) was characterized by the presence of a sudden slope change at about 23 mN/m , probably due to a collapse of the mixed film. At surface pressures between 27 and 44 mN/m the spreading

TABLE 1: Surface Area Occupied by the Single Components in a Spreading Monolayer of the 22/1 (Molecular Ratio) SA/CuR₆R'₂TAP Mixture as a Function of the Surface Pressure

π , mN/m	A (SA), Å ² /molecule calculated	A (SA/CuR ₆ R' ₂ TAP 22/1), Å ² /molecule experimental	A (CuR ₆ R' ₂ TAP), Å ² /molecule calculated	A (CuR ₆ R' ₂ TAP), Å ² /molecule experimental
5	23.6	26.2	83.2	149.6
10	22.8	25.5	84.7	145.6
15	22.0	25.3	97.6	143.0
20	21.5	25.1	104	141.0
25	21.4	22.6	48.9	139.5
30	21.2	20.8	12.0	137.6

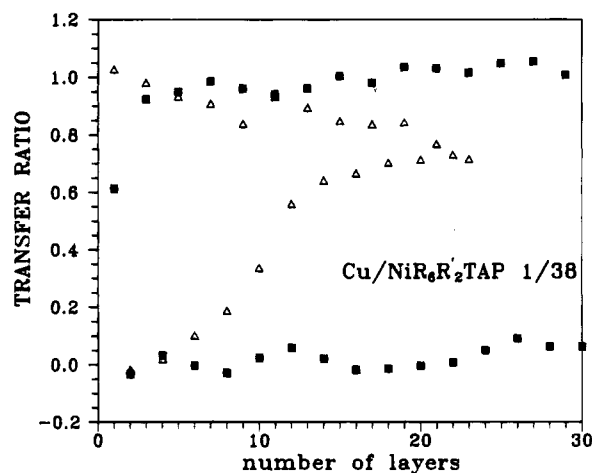
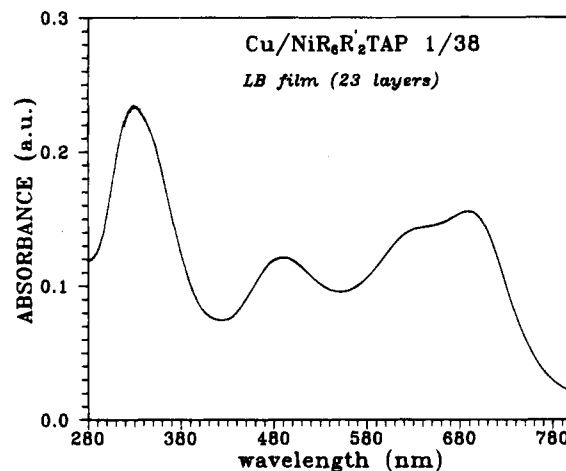
**Figure 7.** Compression–expansion–compression cycles of the same system as in Figure 6.

isotherm was that of the pure matrix compound, as it was clear from the limiting area of 22 Å²/molecule, typical of the stearic acid monolayer. This has also been observed with CuR₈TAP systems.⁹ Table 1 reports the experimental and calculated surface area values for the CuR₆R'₂TAP component in the mixed film at different surface pressures. At $\pi \leq 20$ mN/m the calculated area values for CuR₆R'₂TAP molecules in the mixed system were lower than the value experimentally obtained for the pure CuR₆R'₂TAP monolayer. In the presence of the amphiphilic matrix, the macrocycle assumed an edge-on orientation, more vertical with respect to that in the pure CuR₆R'₂TAP monolayer. Above 20 mN/m the sharp decrease in CuR₆R'₂TAP surface area values indicated a surface transition of the tetraazaporphyrin ring toward a less ordered state.

We also determined compression–expansion–compression cycles on the mixed SA/CuR₆R'₂TAP system (Figure 7). A slight hysteresis was observed in this case too, but it occurred during the second compression only.

The stability curve determined for a time period of 2 h showed a surface area loss of about 4%. The monolayer of this mixture was thus less stable than the previous pure macrocyclic one.

Langmuir–Blodgett Films. The LB film deposition of the Cu/NiR₆R'₂TAP system was possible either on a hydrophilic substrate or on a hydrophobic one. Figure 8 shows the transfer ratio values as a function of the number of layers for both cases. The behavior was strongly dependent on the substrate nature. With hydrophobic quartz the transfer ratio values were almost unity during downstroke and almost zero during upstroke, independent of the number of layers. Decreasing values during downstroke and increasing values during upstroke were observed with hydrophilic quartz. This clearly pushed toward an X-film formation with the hydrophobic substrate, whereas Y-type films were favored with the hydrophobic substrate after the first 20 layers were deposited. The SA/CuR₆R'₂TAP 22/1 system gave good LB films only by depositing the monolayers on hydrophobic substrates.

**Figure 8.** Transfer ratios as a function of the number of layers for the film of Cu/NiR₆R'₂TAP (atomic ratio 1/38) on hydrophobic quartz (■) and on hydrophilic quartz (Δ).**Figure 9.** Electronic spectrum at room temperature of the Langmuir–Blodgett film (23 layers) fabricated with Cu/NiR₆R'₂TAP.

LB films were characterized by UV–vis spectroscopy with both isotropic and polarized light. The same electronic spectra were obtained independently of X- and Y-type deposition. The spectrum of a LB film (23 layers) of the Cu/NiR₆R'₂TAP system (Figure 9) was characterized by the Soret band at 330 nm and a band at 490 nm, at the same wavelengths as in fluid solution. These bands were broader than in solution, which is typical of *quasi* solid spectra. A significant difference between solution and solid spectra was observed in the 560–750 nm range, where the Q bands, typical of tetraazaamcrocyclic rings, occur. The solution absorptions at 670 nm with the shoulder at 610 nm were shifted to 690 and 627 nm, respectively, as is usually observed for porphyrins which have a transition from fluid to solid phase.^{22–24} Moreover, all of the absorption bands were broadened, which indicated a large degree of molecular interactions. The intensity ratio between the two absorptions underwent a sudden increase on going from solution to LB film. Thus,

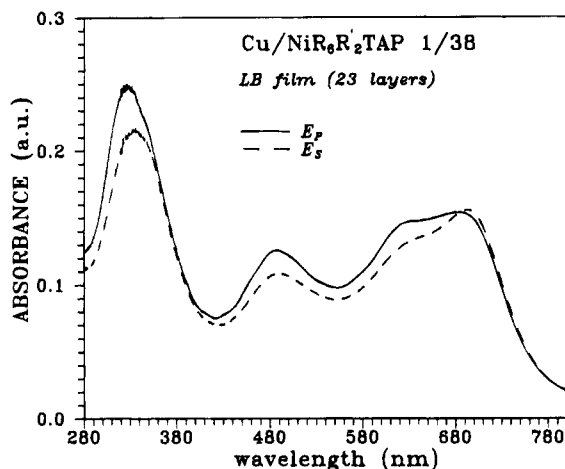


Figure 10. Electronic spectrum in polarized light of the Langmuir-Blodgett film (23 layers) fabricated with Cu/NiR₆R'₂TAP: (solid line) electric field vector parallel to the incidence plane; (dashed line) electric field vector perpendicular to the incidence plane.

TABLE 2: Dichroic Ratios of the Absorption Bands of CuR₆R'₂TAP in the Langmuir-Blodgett Films

sample	328 nm	488 nm	623 nm	689 nm
Cu/NiR ₆ R' ₂ TAP 1/38, 23 layers, $i = 0^\circ$	1.16	1.16	1.13	0.99
Cu/NiR ₆ R' ₂ TAP 1/38, 30 layers, $i = 0^\circ$	1.23	1.27	1.24	1.02

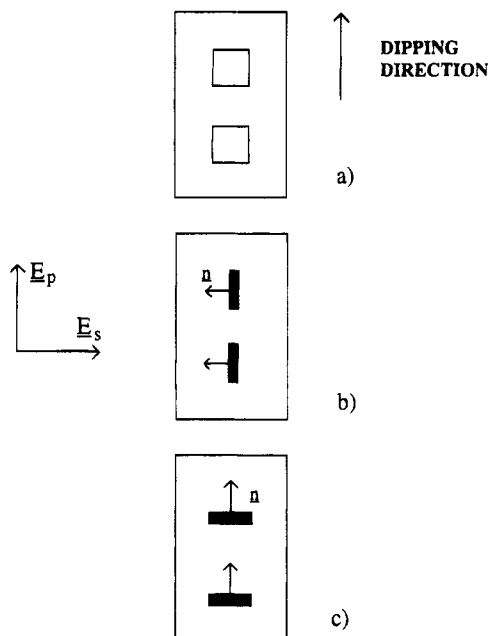


Figure 11. Possible orientation of the TAP macrocycles on the substrate plane: (top) flat orientation ($A(E_p) = A(E_s) = 1$; dichroic ratio = 1); (center) edge-on orientation to the substrate plane with the normal n of the macrocycle perpendicular to the dipping direction ($A(E_p) < A(E_s)$; $R < 1$); (bottom) edge-on orientation to the substrate plane with the normal n of the macrocycle parallel to the dipping direction ($A(E_p) > A(E_s)$; $R > 1$).

the higher energy absorption was not simply due to the vibronic transition Q(1,0), which gave rise to the shoulder in solution. We attribute this absorption to the formation of surface TAP aggregates. It is well-known that phthalocyanine and porphyrin dimer formation results in a blue-shift of the absorption bands with respect to the monomer peak.

The same sample was also investigated with polarized light by using the light polarization plane, E , parallel (E_p) or

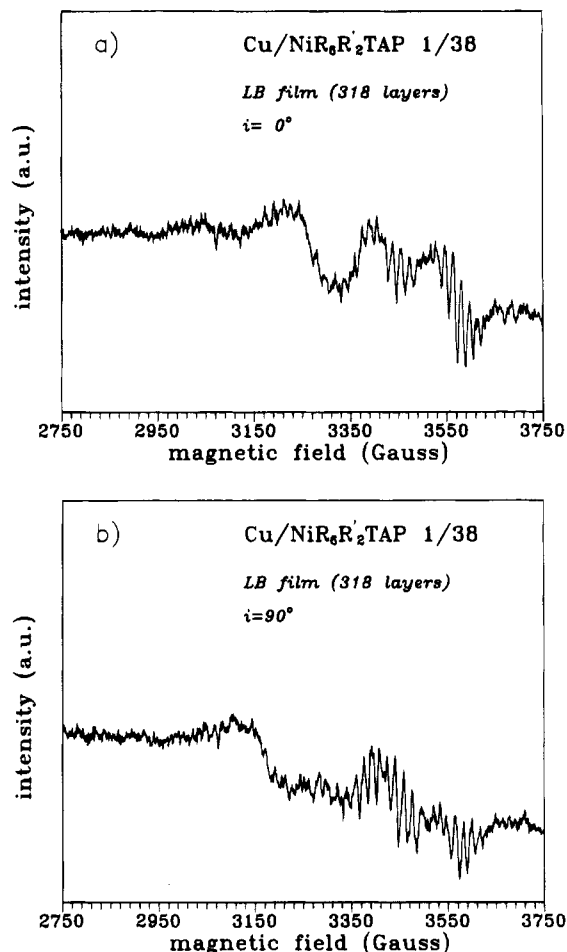


Figure 12. ESR spectra at room temperature of a Langmuir-Blodgett film (318 layers) built up with Cu/NiR₆R'₂TAP monolayers: i represents the angle between the substrate plane and the magnetic field direction.

perpendicular (E_s) to the incidence plane of radiation and at an incidence angle $i = 0^\circ$ of the light beam with respect to the plane normal. The dependence of the absorption bands on the direction of the electric field vector with respect to the dipping direction is shown in Figure 10. The dichroic ratios $R = A(E_p)/A(E_s)$ calculated from the absorption bands are reported in Table 2. The dichroic ratio > 1.0 (calculated for the 328, 488, and 623 nm absorptions) indicated that some molecule order was present within the film. Figure 11 shows three possible orientations of the rings with respect to the dipping direction. With molecules flat on the substrate (case a of Figure 11) no polarization dependence of the light absorption would be expected because the absorption bands are polarized in the xy plane. Dichroic ratios less than 1 were expected with edge-on orientated molecules with the normal to the molecular plane perpendicular to the dipping direction (case b). Finally, dichroic ratios higher than 1 were expected when edge-on-oriented molecules had the normal to the molecular ring parallel to the dipping direction (case c). Our results pointed to case c. The transfer ratios very close to unity further demonstrated that during the LB film deposition a change in molecular orientation did not occur on going from the water surface to the solid substrate.

On the contrary, no polarization effects were observed with films fabricated with the SA/CuR₆R'₂TAP mixture. The same UV-vis spectra were registered with isotropic and polarized light.

The ESR spectra of the Cu/NiR₆R'₂TAP system, at two different orientations of the substrate with respect to the static

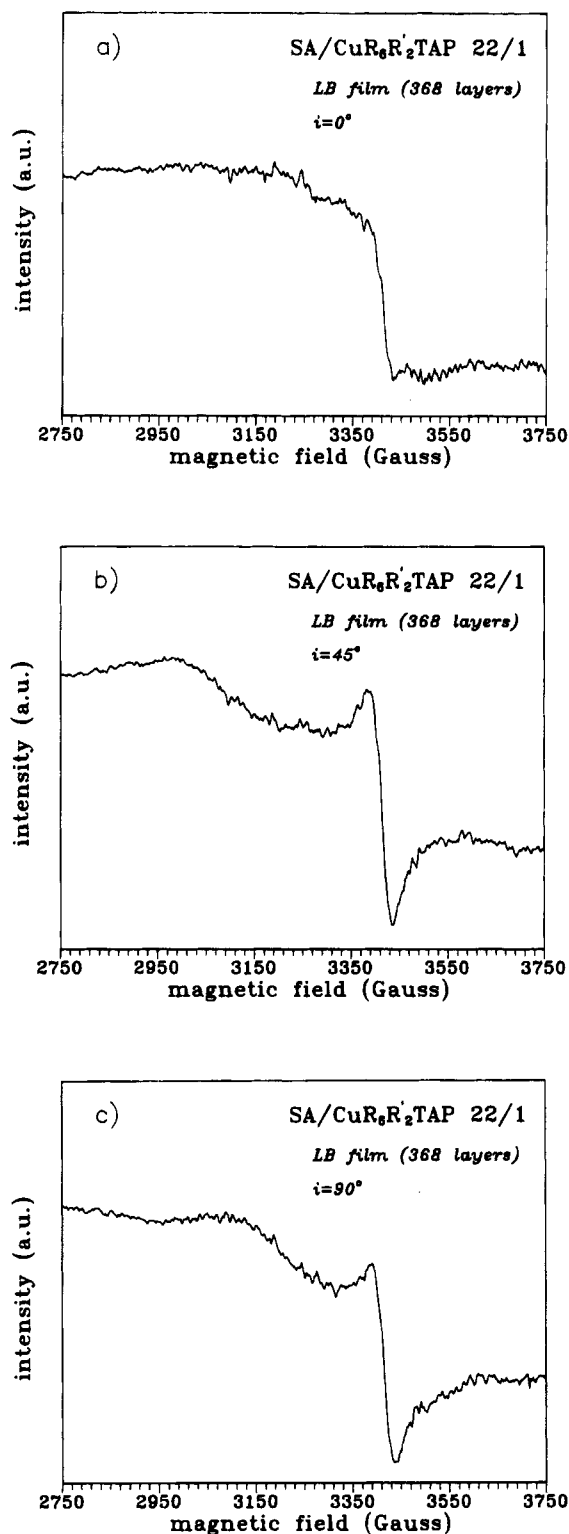


Figure 13. ESR spectra at room temperature of a Langmuir–Blodgett film (368 layers) built up with the SA/CuR₆R'₂TAP (22/1 molecular ratio) mixed monolayers: *i* represents the angle between the substrate plane and the magnetic field direction.

magnetic field, are shown in Figure 12. These spectra were registered from X-type films. The same species responsible for the spectrum reported in Figure 2 appeared, as evidenced from the two high-field manifolds with a partial resolution of the ¹⁴N superhyperfine structure. This spectral component did not seem to show any dependence on the orientation of the normal to the substrate with respect to the static magnetic field. On the contrary, a non-negligible dependence was observed for

an additional broad, unstructured signal. We may suggest that the powder-like spectrum could be due to a small fraction of molecules dispersed in a random way in the matrix of the diamagnetic nickel derivatives. An ordered fraction of the pure copper derivative gave the ESR unresolved absorption. Similar ESR line shapes are observed in LB films of the symmetrically substituted CuR₆TAP diluted in the free base.⁹ In that case neither component was orientation dependent and both species responsible for the absorptions are in an almost completely disordered state. As an alternative interpretation two sets of differently oriented CuR₆R'₂TAP molecules give similar spectral behavior. This situation is approached by Azumi *et al.*,²⁵ who report ESR spectra from tetrakis(3,5-di-*tert*-butylphenyl)porphyrinato copper(II) in LB films due to the same species with different orientation with respect to the substrate. These authors do not observe any ¹⁴N superhyperfine structure, while this structure has been reported in other cases, e.g. by Porteu *et al.*²⁶ for a flat porphyrinato copper(II) LB film. Azumi *et al.*²⁵ have been able to simulate the complex line shape with an optimization of the magnetic parameters. This procedure would certainly aid in solving problems of orientation also in our spectra. However, the very weak intensity of these spectra and the fact that they were obtained from very thick samples whose homogeneity was not warranted may give a very scarce meaning to these procedures. We are now trying to obtain LB films whose spectra overcome the above difficulties in order to simulate correctly their shape.

The ESR spectra for the SA/CuR₆R'₂TAP system are shown in Figure 13. Two difficult absorptions were again responsible for the observed ESR patterns: a single, exchange-narrowed, ESR absorption at high field with a line width of 5.3 mT, due to highly interacting CuR₆R'₂TAP molecules, without any orientation dependence and a broad, unresolved signal, which was slightly orientation dependent. The presence of stearic acid in the mixture did not improve molecular order in the LB film and favored a disordered aggregation of the macrocycles.

Conclusions

The results reported in this work represent a significant improvement in the preparation of thin films of metal derivatives of the tetraazaporphyrin cycle whose properties can be of much use in fabricating LB films. Such LB films can show unusual properties such as, for example, high sensitivity toward environmental gases. The simple unsymmetrization of the substitution around the macrocycle changed neither stability nor homogeneity of the spreading monolayers, whereas it introduced a large fraction of ordered material, as shown by UV–vis and ESR spectroscopies.

Acknowledgment. G.R. thanks Mr. C. Barlabà for technical support. Thanks are due to Italian Ministero della Università e della Ricerca Scientifica e Tecnologica (MURST) and to Consiglio Nazionale delle Ricerche (CNR) for financial support.

References and Notes

- (1) Cook, M. J.; Daniel, M. F.; Harrison, K. J.; McKeown, N. B.; Thomson, A. J. *J. Chem. Soc., Chem. Commun.* **1987**, 1148.
- (2) McKeown, N. B.; Cook, M. J.; Thomson, A. J.; Harrison, K. J.; Daniel, M. F.; Richardson, R. M.; Roser, S. J. *Thin Solid Films* **1988**, *159*, 469.
- (3) Cook, M. J.; McKeown, N. B.; Simmons, J. M.; Thomson, A. J.; Daniel, M. F.; Harrison, K. J.; Richardson, R. M.; Roser, S. J. *J. Mater. Chem.* **1991**, *1*, 121.
- (4) Piechocki, C.; Simon, J.; Scoulios, A.; Guillon, D.; Weber, P. *J. Am. Chem. Soc.* **1982**, *104*, 5245.
- (5) Lelj, F.; Morelli, G.; Ricciardi, G.; Roviello, A.; Sirigu, A. *Liq. Cryst.* **1992**, *12*, 941.

- (6) Markovitsi, D.; Lecuyer, I.; Simon, J. *J. Phys. Chem.* **1991**, *95*, 3620.
- (7) Gregg, B. A.; Fox, M. A.; Bard, A. J. *J. Am. Chem. Soc.* **1989**, *111*, 3024.
- (8) Morelli, G.; Ricciardi, G.; Roviello, A. *Chem. Phys. Lett.* **1991**, *185*, 486.
- (9) Bonosi, F.; Ricciardi, G.; Lelj, F.; Martini, G. *J. Phys. Chem.* **1993**, *97*, 9181.
- (10) Jones, R.; Tredgold, R. H.; Hodge, P. *Thin Solid Films* **1983**, *99*, 25.
- (11) Tredgold, R. H.; Evans, S. D.; Hodge, P.; Jones, R.; Stocks, N. G.; Young, M. C. *J. Brit. Polym. J.* **1987**, *19*, 397.
- (12) Tredgold, R. H.; Evans, S. D.; Hodge, P.; Hoorfar, A. *Thin Solid Films* **1989**, *160*, 99.
- (13) Ogawa, K.; Kinoshita, S.; Yonehara, S.; Nakahara, H.; Fukuda, K. *J. Chem. Soc., Chem. Commun.* **1989**, 477.
- (14) Schramm, C. J.; Hoffman, B. M. *Inorg. Chem.* **1980**, *19*, 383.
- (15) Gouterman, M. In *The Porphyrins, Vol. III: Physical Chemistry*; Dolphin, D., Ed.; Academic Press: New York, 1978; Part A., p 1.
- (16) Lin, W. C. In *The Porphyrins*; Dolphin, D., Ed.; Academic Press: New York, 1979; Vol. 4, Part B.
- (17) André, J.-J.; Berbard, M.; Piechocki, C.; Simon, J. *J. Phys. Chem.* **1986**, *90*, 1327.
- (18) Guzy, C. M.; Raynor, J. B.; Symons, M. C. R. *J. Chem. Soc. A* **1969**, 2299.
- (19) Brown, T. G.; Pedersen, J. L.; Lozos, G. P.; Anderson, J. R.; Hoffman, B. M. *Inorg. Chem.* **1977**, *16*, 1563.
- (20) Harrison, S. E.; Assour, J. M. *J. Chem. Phys.* **1964**, *40*, 365.
- (21) Raynor, J. B.; Robson, M.; Torrens-Barton, S. M. *J. Chem. Soc.* **1977**, 2370.
- (22) Weigh, J. W. *J. Mol. Spectrosc.* **1957**, *1*, 216.
- (23) Boham, J. S.; Gouterman, M.; Howell, B. B. *J. Lumin.* **1975**, *10*, 295.
- (24) Schmehl, R. H.; Shaw, G. L.; Whitten, D. G. *Chem. Phys. Lett.* **1978**, *58*, 549.
- (25) Azumi, R.; Matsumoto, M.; Kawabata, Y.; Kuroda, S.; Sugi, M.; King, L. K.; Crossley, M. J. *J. Phys. Chem.* **1993**, *97*, 12862.
- (26) Porteu, F.; Palacin, S.; Ruaudel-Teixier, A.; Barraud, A. *J. Phys. Chem.* **1991**, *95*, 7438.